Soft landing control strategy for biped robot

Hongbo Zhu
Department of Automation, University of Science and Technology of China, Hefei, China, and
Minzhou Luo, Jianghai Zhao and Tao Li
Institute of Advanced Manufacturing Technology, Hefei Institute of Physical Science,
Chinese Academy of Sciences, Changzhou, China

Abstract

Purpose – The purpose of this paper was to present a soft landing control strategy for a biped robot to avoid and absorb the impulsive reaction forces (which weakens walking stability) caused by the landing impact between the swing foot and the ground.

Design/methodology/approach – First, a suitable trajectory of the swing foot is preplanned to avoid the impulsive reaction forces in the walking direction. Second, the impulsive reaction forces of the landing impact are suppressed by the on-line trajectory modification based on the extended time-domain passivity control with admittance causality that has the reaction forces as inputs and the decomposed swing foot's positions to trim off the forces as the outputs.

Findings – The experiment data and results are described and analyzed, showing that the proposed soft landing control strategy can suppress the impulsive forces and improve walking stability.

Originality/value – The main contribution is that a soft landing control strategy for a biped robot was proposed to deal with the impulsive reaction forces generated by the landing impact, which enhances walking stability.

Keywords Biped robot, Landing impact, Soft landing control, Time-domain passivity control

Paper type Research paper

1. Introduction

In the biped robot research area, many great achievements have been gained in many key technical issues such as biped robot modeling, walking pattern generation and dynamical balance control. For biped robot modeling and walking pattern generation, Kajita *et al.* (2001) proposed a simple model called three-dimensional (3D) linear inverted pendulum model for biped walking pattern generation. Motoi *et al.* (2009) used the virtual linear inverted pendulum model to generate the biped walking pattern. Sato *et al.* (2011) and Shimmyo *et al.* (2013) proposed real-time walking pattern generation method using three-mass models at constant body height. Huang *et al.* (2001) proposed a walking pattern planning method which includes the ground conditions, dynamic stability constraint and relationship between walking patterns and actuator specifications. For a dynamic balance control, Li *et al.* (2011) realized dynamic balance of biped walking using policy gradient reinforcement learning, Lagrange polynomial interpolation and fuzzy logic. Choi *et al.* (2007) proposed a posture/walking control method based on kinematic resolution of center of mass (CoM) Jacobian. Li *et al.* (2012) proposed a dynamic balance control method using sensor fusion, Kalman filter and fuzzy logic. In these key technical issues, realizing the more stable and reliable biped walking is the most fundamental. During walking, the impulsive reaction forces between the swing foot and the ground weakens the stability and reliability of biped robots seriously. Hence, this paper aims to enhance the stability and reliability of biped walking by avoiding and suppressing the impulsive reaction forces caused by the landing impact between the swing foot of the robot and the ground.

Up to now, researchers have proposed some methods to relieve the impact of the impulsive landing force during the walking for the biped robot. Some of them were proposed to realize the soft landing control through changing the swing foot's positions using proportion integral derivative (PID) control method (Huang *et al.*, 2005; Yamaguchi *et al.*, 1996; Silva *et al.*, 2000). For example, Huang *et al.* (2005) proposed a walk soft landing control method consisting of a feed-forward dynamic pattern and a feedback sensory reflex. These control methods are easy to implement, but troublesome in that PID coefficients must be determined manually (Kim *et al.*, 2007).

Others have proposed to reducing the impulsive landing force using the hybrid impedance control scheme or computed torque feedback control method after solving the complicated dynamical equations of the biped robot and the ground environment (Shibata and Natori, 2000; Park, 2001; Lim *et al.*, 2004). For example, Park (2001) proposed a landing force control method for biped robot locomotion based on

The current issue and full text archive of this journal is available on Emerald Insight at: **www.emeraldinsight.com/0143-991X.htm**

Industrial Robot: An International Journal
44/3 (2017) 312–323

[DOI 10.1108/IR-09-2016-0244]

This research has been supported by National Science and Technology Support Program (Grant No.2015BAK06B02), Science and Technology Support Plan Key Projects of Jiangsu province (Grant No.BE2013003) and National Nature Science Foundation of China (Grant No. 51405469).

Received 22 September 2016
Revised 1 December 2016
Accepted 5 December 2016

impedance control and impedance modulation. Although control parameters can be determined mathematically, complicated dynamical equations need high computation cost and the parameters also need be regulated according to the walking condition (Kim *et al.*, 2007).

Then, Kim and others proposed a landing force control based on time-domain passivity approach (Hannaford and Ryu, 2002; Ryu *et al.*, 2004) to compensate the landing force of a biped robot (Kim *et al.*, 2007). The method does not need any parameters to be tuned and determined, and also, a complex and special foot structure is not needed. However, the above-mentioned methods were proposed to suppress the impulsive landing force in the normal direction of the flat terrain [Figure 1(a)] without consideration of the impulsive forces in the other directions. Furthermore, these methods are useless to slope and uneven terrain, as shown in Figure 1.

So, this paper details a soft landing control strategy to avoid and suppress the impulsive ground reaction forces for enhancing the biped walking stability. The control strategy is composed of two parts. The first one is planning a suitable trajectory of the swing foot in advance to avoid the impulsive reaction force along the walking direction. The other one is on-line modification of the preplanned trajectories of the swing foot and COM for absorbing the impulsive reaction forces. For the on-line modification part, this paper has extended the one-port network system with admittance causality that is the model of the swing foot and the ground in reference (Kim *et al.*, 2007) to the three-ports network system with admittance causality used as the improved novel model of the swing foot and the ground, as shown in Figure 2. By calculating the energy inputs into the three-ports network based on the landing forces and the foot positions, the biped robot's foot is controlled to be passive.

The organization of this paper is as follows. In Section 2, the method for trajectory planning of the swing foot is demonstrated in detail. In Section 3, the on-line modification method based on the extended time-domain passivity and the three-ports network model system for absorbing the impulsive reaction forces has been described. In Section 4, the experiment results have been presented and the effectiveness of the soft landing control strategy is demonstrated. Conclusions are drawn in Section 5.

Figure 2 Three-ports network model

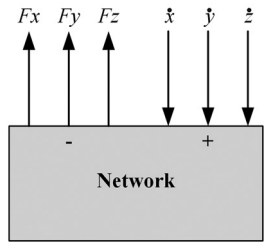

2. Trajectory planning of the swing foot

The trajectories of the swing foot can cause a tipping moment on the biped robot because of the reaction forces generated by the impact against the ground or the inertial force that appears when the foot is accelerated. The caused inertial force also reduces the effectiveness for tracking the commanded positions of the joint actuators seriously. The degree of the reaction forces exerted by the impact between the swing foot and the ground depends on the instantaneous velocity of the swing foot at the time of touching the ground. This velocity can be composed into two components. The first one, v_{pb}, is parallel to the body plane, the other one, v_{nb}, is normal to the body plane. The components of the reaction force in the direction of the body plane, f_{pb}, and in the normal direction of the body plane, f_{nb}, have something to do with the components of swing foot velocity v_{pb} and v_{nb}, respectively, $f_{pb} = f(v_{pb})$ and $f_{nb} = f(v_{nb})$. The moment generated by the component f_{nb} of the reaction force will accelerate the tipping over. Hence, a good strategy for reducing the impulsive reaction force caused by f_{nb} is to make v_{nb} reach and keep zero before v_{pb} by planning suitable trajectory of the swing foot. In other words, the swing foot reaches the destination in the normal direction of the body plane before the direction of the body plane. Hence, the swing foot trajectory in the world frame for $t \in [0, T]$ can be planned as:

$$x_{sf} = S_{stride}\left(\frac{t}{\delta T} - \frac{\sin\left(\frac{2\pi t}{\delta T}\right)}{2\pi}\right) \quad (1)$$

Figure 1 The sights of the landing on various terrains of the swing foot of a biped robot

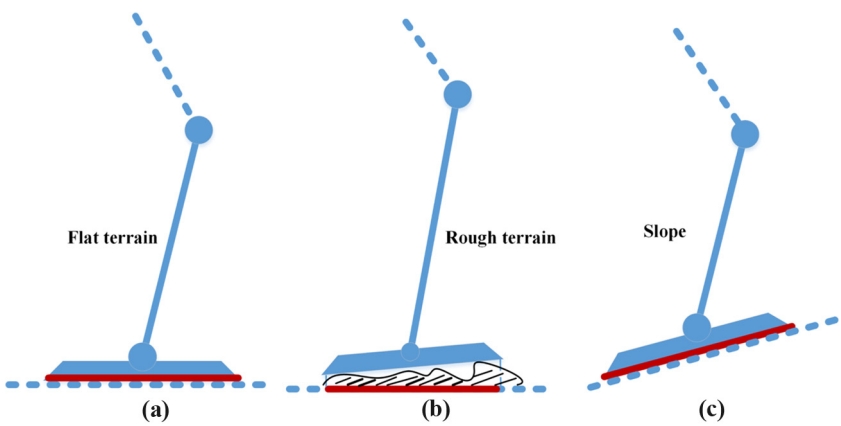

$$y_{sf} = (-1)^n W \tag{2}$$

$$z_{sf} = H_{step}/2\left(1 - \cos\left(\frac{\pi t}{2T}\right)\right) \quad \text{for } t \in [0,\ T/2] \tag{3}$$

$$z_{sf} = (H_{step} + h)/2\left(1 - \cos\left(\frac{\pi t}{2T}\right)\right) \quad \text{for } t \in [T/2,\ T] \tag{4}$$

where S_{stride} is the stride of the biped robot in the walking direction; H_{step} is foot clearance which is the maximum step height during foot swing; W is the step width; n is the step number; h is the changing height of the terrain; T is the whole duration of the step; and δ is the proportionality coefficient of the whole duration, which usually is set to 0.9 considering the limitation of accelerations. Figure 3 shows, in sagittal plane, the trajectory design selected for standard forwards walking. The trajectory planning approach with $\delta = 0.9$, as shown in Figure 3, can avoid the impulsive reaction force caused by f_{nb}; allows online modification of the swing foot position considering disturbances or minor errors; and provides flexibility to generate complex trajectories.

3. On-line modification based on extended time-domain passivity control

3.1 Extended time-domain passivity

In this section, the extended time-domain passivity concept has been demonstrated briefly. To make it be used for absorbing the impulsive landing forces during walking, we have extended the time-domain passivity concept simply. The definition of extended time-domain passivity is as given below.

The three-ports network with initial energy storage $\mathbf{E}(0) = [E_x(0)\ E_y(0)\ E_z(0)]^T$ is continuous time passive if and only if:

$$\boldsymbol{E}(t) = \begin{bmatrix} E_x(t) \\ E_y(t) \\ E_z(t) \end{bmatrix} = \begin{bmatrix} \int_0^t F_x(\tau)\dot{x}(\tau)d\tau \\ \int_0^t F_y(\tau)\dot{y}(\tau)d\tau \\ \int_0^t F_z(\tau)\dot{z}(\tau)d\tau \end{bmatrix} + \mathbf{E}(0) \geq 0 \quad \forall\, t \geq 0 \tag{5}$$

for force $\boldsymbol{F} = [F_x\ F_y\ F_z]^T$ and velocity $\dot{\boldsymbol{p}} = [\dot{x}\ \dot{y}\ \dot{z}]^T$.

Figure 3 Swing foot trajectories in the sagittal plane for standard forwards walking

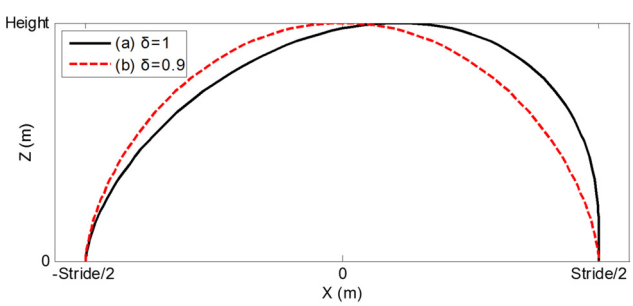

Notes: (a) Corresponds to $\delta = 1$; (b) $\delta = 0.9$

In consideration of that the robot control system is the sampled time system, the corresponding passivity of the sampled time system can be defined as following:

The three-ports network with initial energy storage $\mathbf{E}(0) = [E_x(0)\ E_y(0)\ E_z(0)]^T$ is sampled time passive if and only if:

$$\boldsymbol{E}(t_k) = \begin{bmatrix} E_x(t_k) \\ E_y(t_k) \\ E_z(t_k) \end{bmatrix} = \begin{bmatrix} \sum_{j=0}^{k} F_x(t_j)(x(t_j) - x(t_{j-1})) \\ \sum_{j=0}^{k} F_y(t_j)(y(t_j) - y(t_{j-1})) \\ \sum_{j=0}^{k} F_z(t_j)(z(t_j) - z(t_{j-1})) \end{bmatrix} + \mathbf{E}(0) \geq \mathbf{0} \tag{6}$$

where $j = 0, 1, 2, \cdots, k$ and $k = 0, 1, 2, \cdots$ for sampled force $\boldsymbol{F}(t_k) = [F_x(t_k)\ F_y(t_k)\ F_z(t_k)]^T$ and position $\boldsymbol{p}(t_k) = [x(t_k)\ y(t_k)\ z(t_k)]^T$.

3.2 Biped robot's foot and the ground modeling

The biped robot's configuration and coordinates are illustrated in Figures 4 and 5. $\sum_W$ is the world coordinates frame, and $\sum_G$ is the ground coordinates frame. In the flat terrain, $\sum_G$ and $\sum_W$ are the same coordinates frame. In the slope or rough terrain, they are different. The foot's position can be expressed in $\sum_W$ as:

$$\boldsymbol{p}_i^W = \begin{bmatrix} x_i^W & y_i^W & z_i^W \end{bmatrix}^T \quad \text{for} \quad i \in \{L, R\} \tag{7}$$

Figure 4 Biped robot model and configuration model

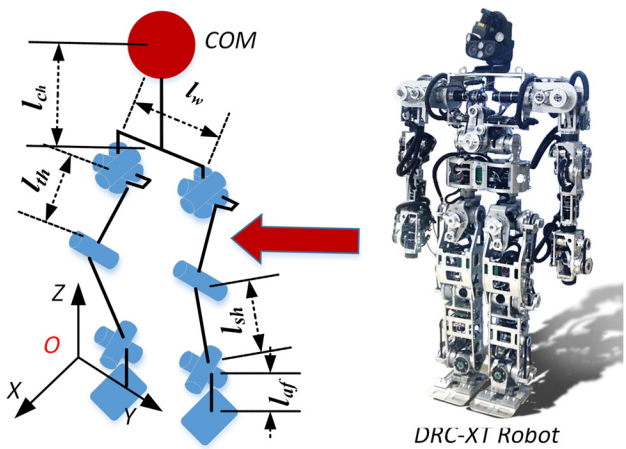

Figure 5 The system model of biped robot foot and the ground

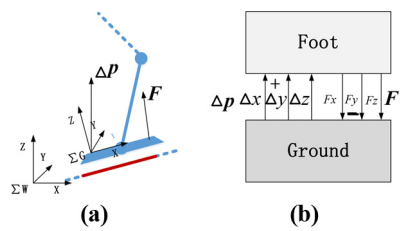

Notes: (a) The foot and the slope ground; (b) the three-ports network system model

in $\sum_G$ as:

$$\boldsymbol{p}_i = [x_i \;\; y_i \;\; z_i]^T \quad \text{for} \quad i \in \{L, R\} \tag{8}$$

where L and R denote the left foot and right foot, respectively, and the biped robot's foot and the ground are modeled as a three-ports network system, as shown in Figure 5, which are connected to each other. In Figure 5, the reaction force $\boldsymbol{F} = [F_x \;\; F_y \;\; F_z]^T$ and the velocity $\Delta\boldsymbol{p}_i$ are expressed in $\sum_G$. The following vectors are all expressed in $\sum_G$ unless noted otherwise. According the equations (5) and (6), the passivity of the three-ports system of biped robot foot and the ground can be expressed as:

$$\boldsymbol{E}(k) = \sum_{j=0}^{k} \begin{bmatrix} F_x(j)(x(j) - x(j-1)) \\ F_y(j)(y(j) - y(j-1)) \\ F_z(j)(z(j) - z(j-1)) \end{bmatrix} + \boldsymbol{E}(0) \geq 0 \tag{9}$$

3.3 Compensation for the landing forces using the extended time-domain passivity control

The three-ports network system, as shown in Figure 5(b), can be divided into two parts, a foot position controller and a planner for generating the walking trajectory (as described in Section 2), as shown in Figure 6. In addition, the extended time-domain passivity control is composed of three passivity observers (POs) monitoring the inputs/outputs energy flows between the foot and the ground and three passivity controllers (PCs) controlling the energy flows.

According to the landing force $\boldsymbol{F} = [F_x \;\; F_y \;\; F_z]^T$ measured by the six-axes force/torque sensor on the biped robot's ankle and the foot position $\boldsymbol{p}_i = [x_i \;\; y_i \;\; z_i]^T$, the energy flows $\boldsymbol{W}(k) = [W_x(k) \;\; W_y(k) \;\; W_z(k)]^T$ between the biped robot foot and the ground can be calculated by the POs:

$$\boldsymbol{W}(k) = \boldsymbol{W}(k-1) + \begin{bmatrix} f_{x1}(k)(x_1(k) - x_1(k-1)) \\ f_{y1}(k)(y_1(k) - y_1(k-1)) \\ f_{z1}(k)(z_1(k) - z_1(k-1)) \end{bmatrix} \tag{10}$$

$$\boldsymbol{W}_o(k+1) = \boldsymbol{W}(k) + \begin{bmatrix} f_{x1}(k)(x_2(k+1) - x_1(k)) \\ f_{y1}(k)(y_2(k+1) - y_1(k)) \\ f_{z1}(k)(z_2(k+1) - z_1(k)) \end{bmatrix} \tag{11}$$

Figure 6 Three-ports network of the system of biped robot's foot and the ground with PO/PCs

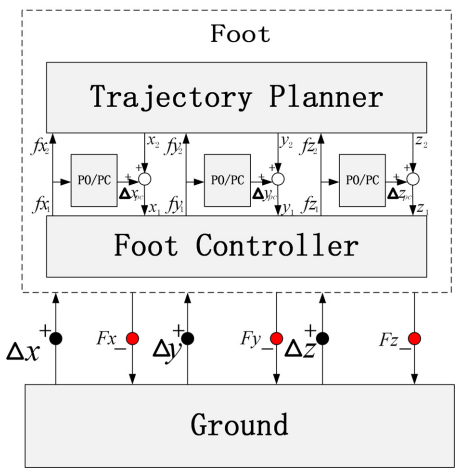

where $\boldsymbol{W}(k)$ is the total energy outputs from 0 to k including the z-axis energy output $W_z(k)$, the y-axis direction energy output $W_y(k)$ and the x-axis direction energy output $W_x(k)$; and $\boldsymbol{W}_o(k+1) = [W_{ox}(k+1) \;\; W_{oy}(k+1) \;\; W_{oz}(k+1)]^T$ is the prediction of the one-step-ahead energy outputs from k to $k+1$.

The desired foot position $\boldsymbol{p}_i$ can be modified at the next step to make the system of the foot and the ground passive by the PCs. The PCs absorb exactly the net energy outputs measured by the POs at each time sample. The PCs algorithm for the three-ports network system can be described as:

- $\boldsymbol{F}_1 = [f_{x1} \;\; f_{y1} \;\; f_{z1}]^T = \boldsymbol{F}_2 = [f_{x2} \;\; f_{y2} \;\; f_{z2}]^T$ are the inputs.
- $\Delta\boldsymbol{p}_1(k) = \boldsymbol{p}_1(k) - \boldsymbol{p}_1(k-1) = [x_1(k)y_1(k)z_1(k)]^T - [x_1(k-1)y_1(k-1)z_1(k-1)]^T \quad \Delta\boldsymbol{p}_2(k+1) = \boldsymbol{p}_2(k+1) - \boldsymbol{p}_1(k) = [x_2(k+1) \;\; y_2(k+1) \;\; z_2(k+1)]^T - [x_1(k) \; y_1(k) \; z_1(k)]^T$
- $\Delta\boldsymbol{p}_2(k)$ are the outputs of the three-ports network.
- $\boldsymbol{W}(k) = \boldsymbol{W}(k-1) + \begin{bmatrix} f_{x1}(k)\Delta x_1(k) \\ f_{y1}(k)\Delta y_1(k) \\ f_{z1}(k)\Delta z_1(k) \end{bmatrix}$ are the energy outputs in different directions at the step k.
- $\boldsymbol{W}_o(k+1) = \boldsymbol{W}(k) + \begin{bmatrix} f_{x1}(k)\Delta x_2(k+1) \\ f_{y1}(k)\Delta y_2(k+1) \\ f_{z1}(k)\Delta z_2(k+1) \end{bmatrix}$ are the prediction of the energy outputs at the step $k+1$ in different directions.
- The PCs outputs $\Delta\boldsymbol{p}_{pc}(k) = [\Delta x_{pc}(k) \;\; \Delta y_{pc}(k) \;\; \Delta z_{pc}(k)]^T$ for making the system passive are calculated as:

$$\Delta x_{pc}(k) = \begin{cases} -\lambda \dfrac{W_{ox}(k+1)}{f_{x1}(k)}, & \text{if } W_{ox}(k+1) < 0 \\ 0, & \text{if } W_{ox}(k+1) \geq 0 \end{cases}$$

$$\Delta y_{pc}(k) = \begin{cases} -\mu \dfrac{W_{oy}(k+1)}{f_{y1}(k)}, & \text{if } W_{oy}(k+1) < 0 \\ 0, & \text{if } W_{oy}(k+1) \geq 0 \end{cases}$$

$$\Delta z_{pc}(k) = \begin{cases} -\nu \dfrac{W_{oz}(k+1)}{f_{z1}(k)}, & \text{if } W_{oz}(k+1) < 0 \\ 0, & \text{if } W_{oz}(k+1) \geq 0 \end{cases}$$

where λ, μ, $\nu \in (-0, 1]$ are the compensation coefficient of proportionality.

- The stable boundary limits the PCs outputs as follows:

$$\Delta x_{pc} = \Delta x_{pc\_MAX}, \quad \text{if } \Delta x_{pc} > \Delta x_{pc\_MAX}$$

$$\Delta y_{pc} = \Delta y_{pc\_MAX}, \quad \text{if } \Delta y_{pc} > \Delta y_{pc\_MAX}$$

$$\Delta z_{pc} = \Delta z_{pc\_MAX}, \quad \text{if } \Delta z_{pc} > \Delta z_{pc\_MAX}$$

- The modified desired foot position $\boldsymbol{p}_{i1}(k+1)$ is expressed as $\Delta\boldsymbol{p}_{i1}(k+1) = \Delta\boldsymbol{p}_{i2}(k+1) + \Delta\boldsymbol{p}_{pc}(k)$.

In consideration of the size of biped robot's foot, weight of biped robot's leg and waking speed, the stable boundary Δp_{pc_MAX} should be set appropriately to restrict the PCs outputs, improving the biped robot's walking stability.

3.4 Recover to the original reference trajectory

After the soft landing has been achieved, the biped robot's walking trajectory should be modified for tracking the original reference walking trajectory. To solve this problem, the simplified biped robot model 3D-linear inverted pendulum mode (LIPM), as shown in Figure 4, is considered. The corresponding dynamical equation of the biped robot is described as follows:

$$m(\ddot{p}^W_{COG} + g^W) = F^W$$

$$\ddot{p}^W_{COG} = \frac{F^W}{m} - g^W \tag{12}$$

where $p^W_{COG} = [x^W_{COG} \;\; y^W_{COG} \;\; z^W_{COG}]^T$ is the position of the center of gravity (COG) of biped robot in the world coordinates frame, g^W is the acceleration of the gravity and m is the total mass of biped robot. In the discrete-time system, the equation (12) can be expressed as follow:

$$\Delta p^W_{COG}(k+1) - \Delta p^W_{COG}(k) = \left(\frac{F^W}{m} - g^W\right)T^2 \tag{13}$$

with:

$$\Delta p^W_{COG}(k) \equiv p^W_{COG}(k) - p^W_{COG}(k-1)$$

where T is the sampling time. An error compensation is added to recover the COG trajectory to the desired trajectory, as follows:

$$\Delta p^W_{COG}(k+1) = \Delta p^W_{COG}(k) + \left(\frac{F^W}{m} - g^W\right)T^2 + K\Delta^{Ref}p^W_{COG}(k) + D\Delta^{2Ref}p^W_{COG}(k) \tag{14}$$

with:

$$\Delta^{Ref}p^W_{COG}(k) \equiv p^W_{RefCOG}(k) - p^W_{COG}(k)$$

$$\Delta^{2Ref}p^W_{COG}(k) \equiv \Delta^{Ref}p^W_{COG}(k) - \Delta^{Ref}p^W_{COG}(k-1)$$

Figure 7 The control diagram of the extended time-domain passivity

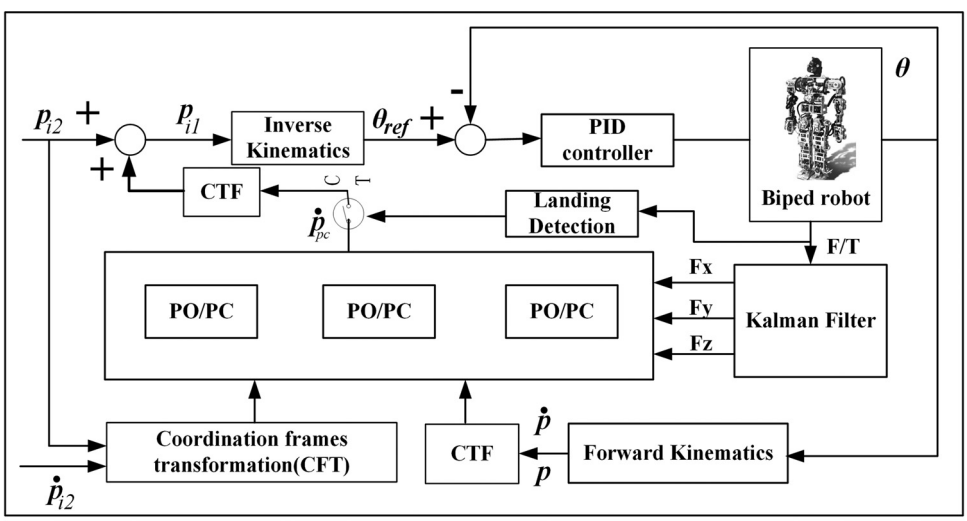

where p^W_{RefCOG} is the pre-planned reference trajectory; and K and D are the proportional and the differential gain, respectively.

Once the soft landing of the swing foot is achieved, the reaction Force F can be expressed as $F^W \approx m[\ddot{x}^W_{RefCOG} \;\; \ddot{y}^W_{RefCOG} \;\; g]$ because of $\ddot{z}^W_{COG} \approx 0$. So, the motion to follow the original trajectory can be obtained as:

$$\Delta p^W_{COG}(k+1) = \Delta p^W_{COG}(k) + T^2\begin{bmatrix}\ddot{x}^W_{RefCOG}(k)\\ \ddot{y}^W_{RefCOG}(k)\\ 0\end{bmatrix} + K\Delta^{Ref}p^W_{COG}(k) + D\Delta^{2Ref}p^W_{COG}(k) \tag{15}$$

Figure 8 The dynamical bipedal walking experiments on the slope terrain and uneven terrain

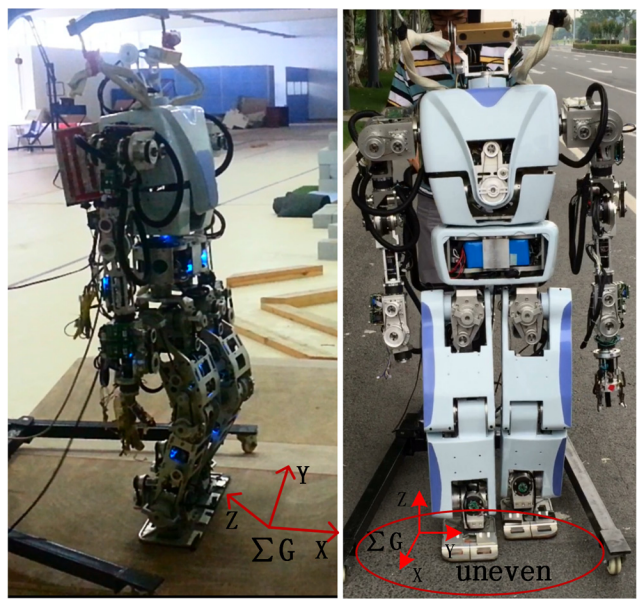

(a) (b)

where $\ddot{x}^{W}_{RefCOG}$ and $\ddot{y}^{W}_{RefCOG}(k)$ are the pre-planned reference acceleration values of COG. In addition, the POs are also reset to prepare the next observation in this stage. In this section, all vectors are expressed in the world coordinates frame $\sum_W$ when they are calculated.

4. Experiments

4.1 Experimental platform and terrain description

DRC-XT humanoid robot developed for Defense Advanced Research Projects Agency (DARPA) Robotics Challenge held by DARPA has 30 degrees of freedom from head to foot, whose leg links are connected by 12 motorized joints and arm links are connected by 14 motorized joints, as shown in Figure 4. The robot controller is an embedded computer with a Pentium 1.6-GHz CPU, 1-GB DDR2 memory and RT-Linux operating system. To measure forces/torques and attitude of the foot, two six-axes force/torque sensors and two attitude sensors are equipped in each ankle.

The extended time-domain passivity control is used in the biped robot DRC-XT, as shown in Figure 7. In the joints space control of biped robots, the motion of the joints is controlled by the PID to track the reference joint trajectory. When the landing forces are detected from the six-axes force/torque sensor, the PO/PCs compensate for the landing force $\boldsymbol{F} = [F_x \;\; F_y \;\; F_z]^T$. Then, the compensated position is added to the pre-planned biped robot's position.

In Figure 8, the dynamical bipedal walking experiments of the biped robot DRC-XT on (a) the slope terrain with an angle of about $\angle 10^o$ and (b) the uneven terrain with different height and grade were conducted to verify the soft landing control strategy. In the walking experiments, the biped robot walked with a step width of 18 cm, a step length of 7.5 cm and a step height of 3 cm in the world coordinates frame $\sum_W$. The COM and swing foot trajectories are planned and expressed in the world coordinates frame $\sum_W$, and the reaction forces and moments measured by the six-axes force/torque sensor are expressed in the foot local coordinates frame, which is parallel to the ground coordinates frame $\sum_G$. So, the preplanned feet

Figure 9 The pre-planned decomposed position trajectories of the feet for the slope

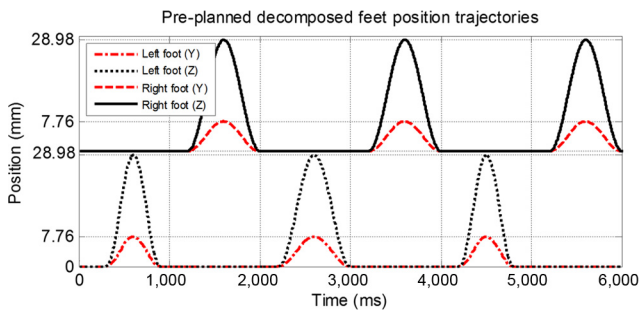

Figure 10 The reaction forces without the on-line modification for the slope

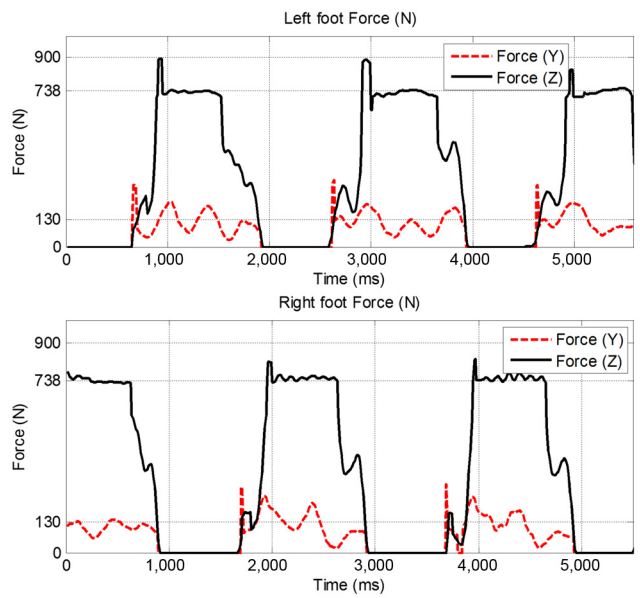

Figure 11 The energy without on-line modification for the slope

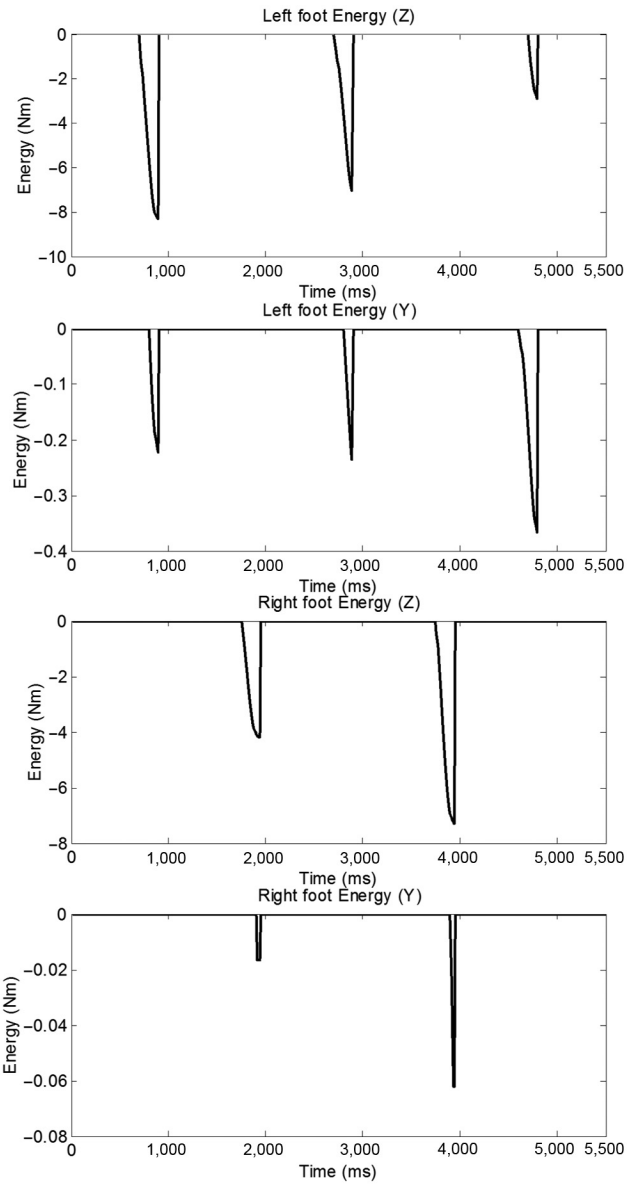

position trajectories in $\sum_W$ need to be decomposed or transformed into $\sum_G$.

4.2 Experimental results and discussion for the slope terrain

For the slope terrain, as shown in Figure 8(a), Figure 9 shows the preplanned decomposed position trajectories (y-axis and z-axis) of the feet expressed in the ground coordinates frame, which decomposed or transformed from the preplanned position trajectories (y-axis and z-axis) expressed in the world coordinates frame. The preplanned y-axis position trajectory in the world coordinates frame is constant, then the decomposed position trajectories (y-axis and z-axis) are also constant in the ground coordinates frame. In addition, the constant offsets do not produce the impulsive impact, so we did not consider the constant offsets in Figure 9.

Figure 10 shows the reaction forces without on-line modification based on extended time-domain passivity control. When the swing foot of the biped robot was landing, there were big landing impulsive forces along the y- and z-axes in the ground coordinates frame. In the z-axis, the maximum value of the landing force was approximate to 900 N. In the y-axis, the maximum value of the landing force was approximate to 318 N. The maximum value of the resultant force of them was approximate to 954.5 N, which was about 1.274 times weight of the biped robot. Figure 11 shows the input energies from the three-ports robot's foot for the slope. When the swing foot was landing, the energy was negative and big, which makes the biped robot walking unstable. Figures 12-15 show the results when on-line modification based on extended time-domain passivity control was used. Compared with the no on-line modification, the proposed control strategy has improved

Figure 12 The reaction forces with on-line modification for the slope

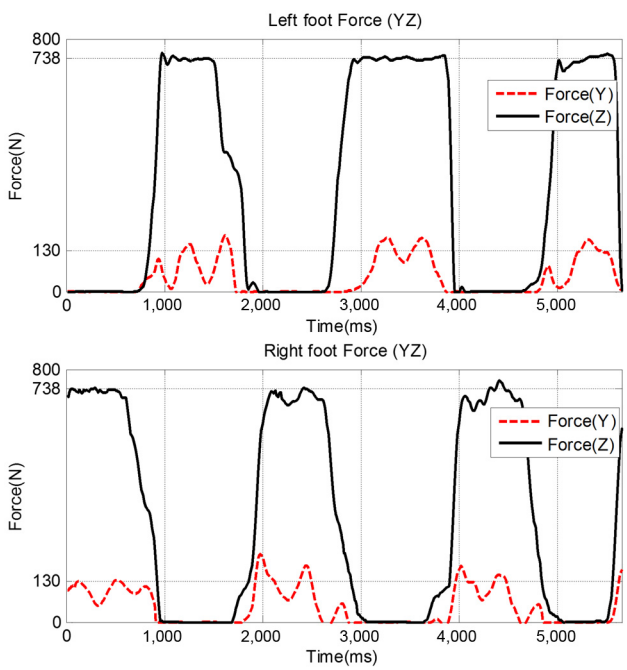

Figure 13 The energy with on-line modification for the slope

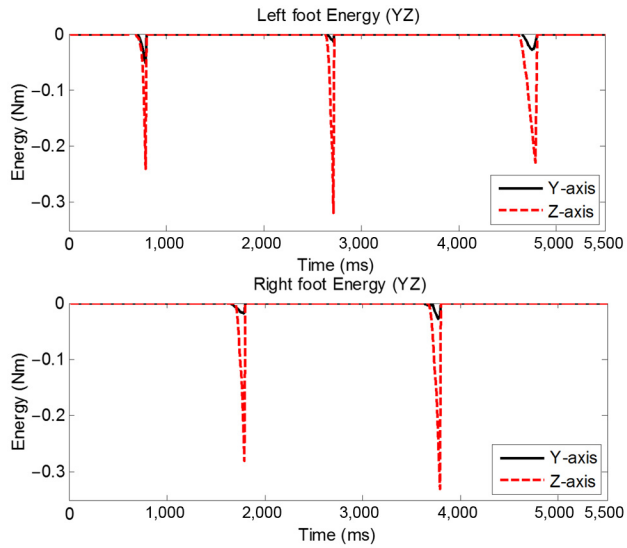

Figure 14 The output of PO/PCs ($\Delta \boldsymbol{p}_{pc}$) by the PO/PCs method for the slope

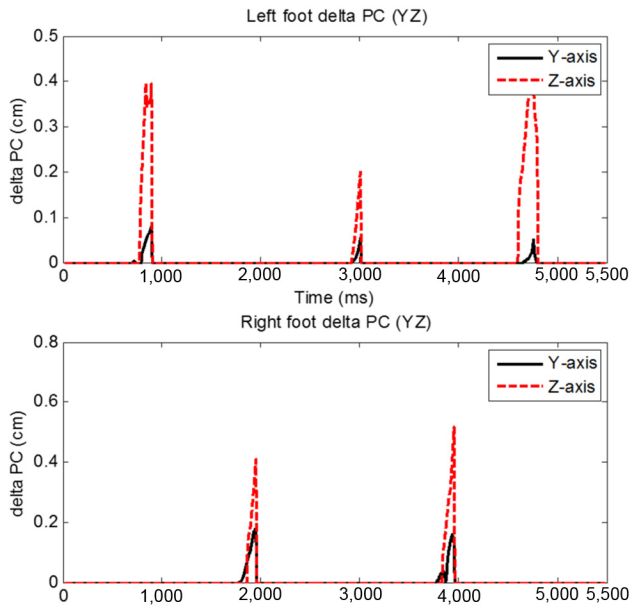

Figure 15 The decomposed position trajectories of the feet with on-line modification for the slope

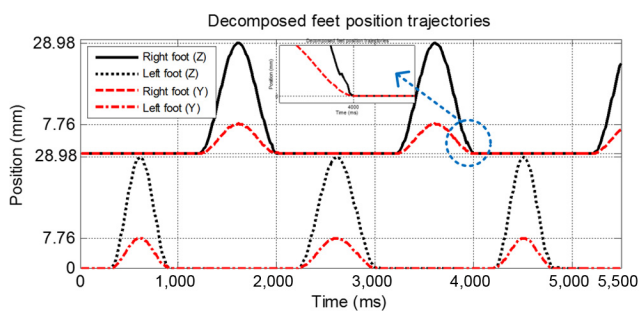

Figure 16 The preplanned position trajectories of the feet for the uneven terrain

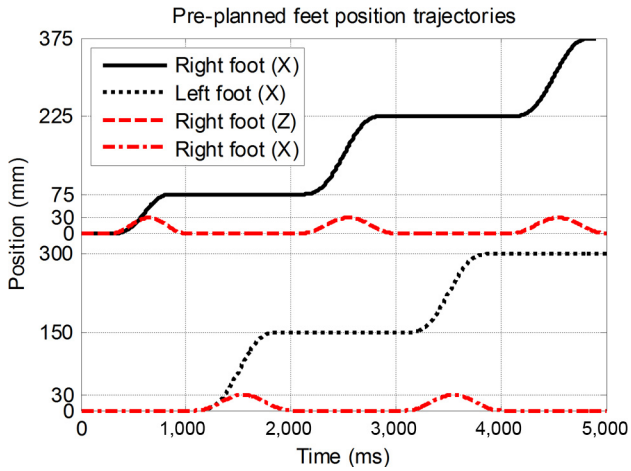

the performance of bipedal walking on the slope. In Figure 12, the impulsive forces had been suppressed well compared with Figure 10 when the swing foot was landing, and the scale of negative energies was decreased by 10-20 times compared to the no on-line modification control, as shown in Figure 11. Figure 14 shows the output $\Delta \boldsymbol{p}_{pc}$ of the PC/POs, which was used to modify the pre-planned position trajectories of the feet. Figure 15 shows the modified decomposed position trajectories of the feet in the ground coordinates frame $\sum_G$.

4.3 Experimental results and discussion for the uneven terrain

For the uneven terrain as shown in Figure 8(b), Figure 16 shows the preplanned position trajectories (x-axis and z-axis) expressed in the world coordinates frame. The constant offsets (y-axis) were also not be considered in Figure 16.

Figure 17 shows the reaction forces without on-line modification. During the walking on the uneven terrain, there were big impulsive forces along the x-axis and z-axis. Along the x-axis, the impulsive force was negative and the

Figure 17 The reaction forces without on-line modification for the uneven terrain

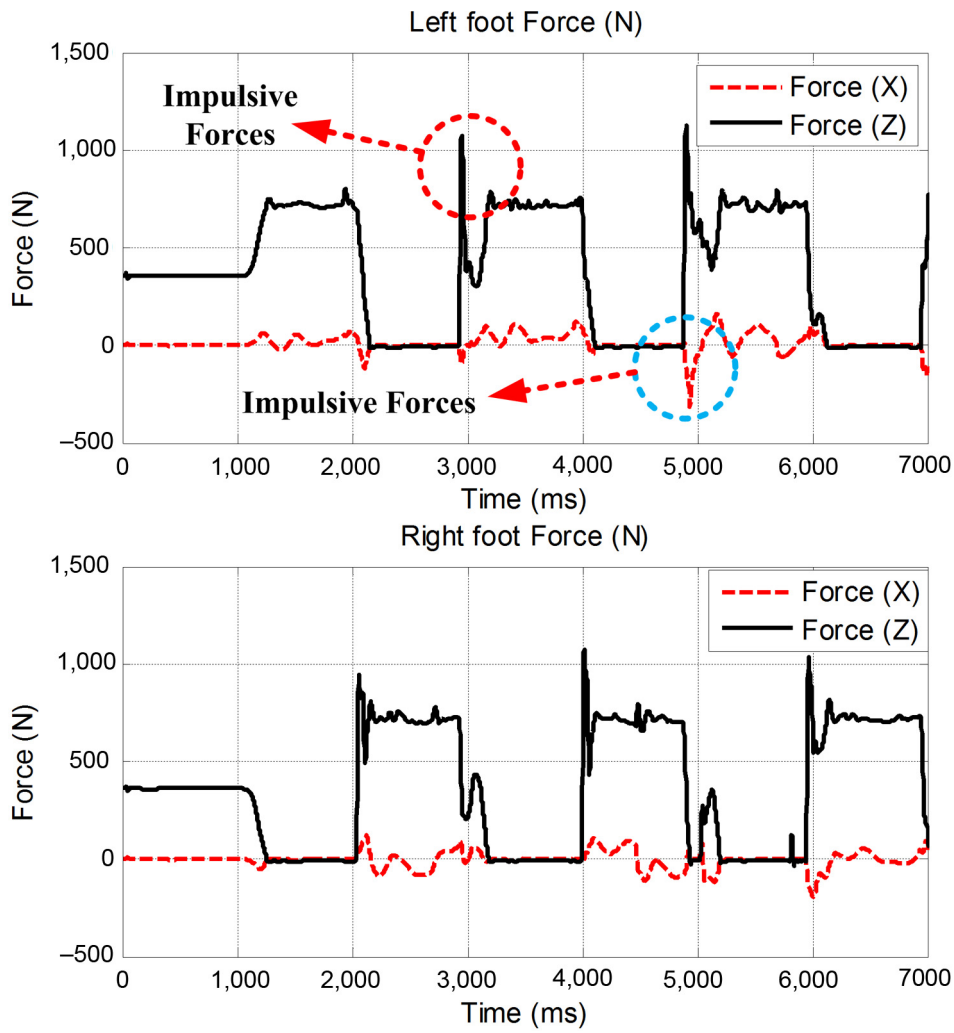

Figure 18 The energy without on-line modification for the uneven terrain

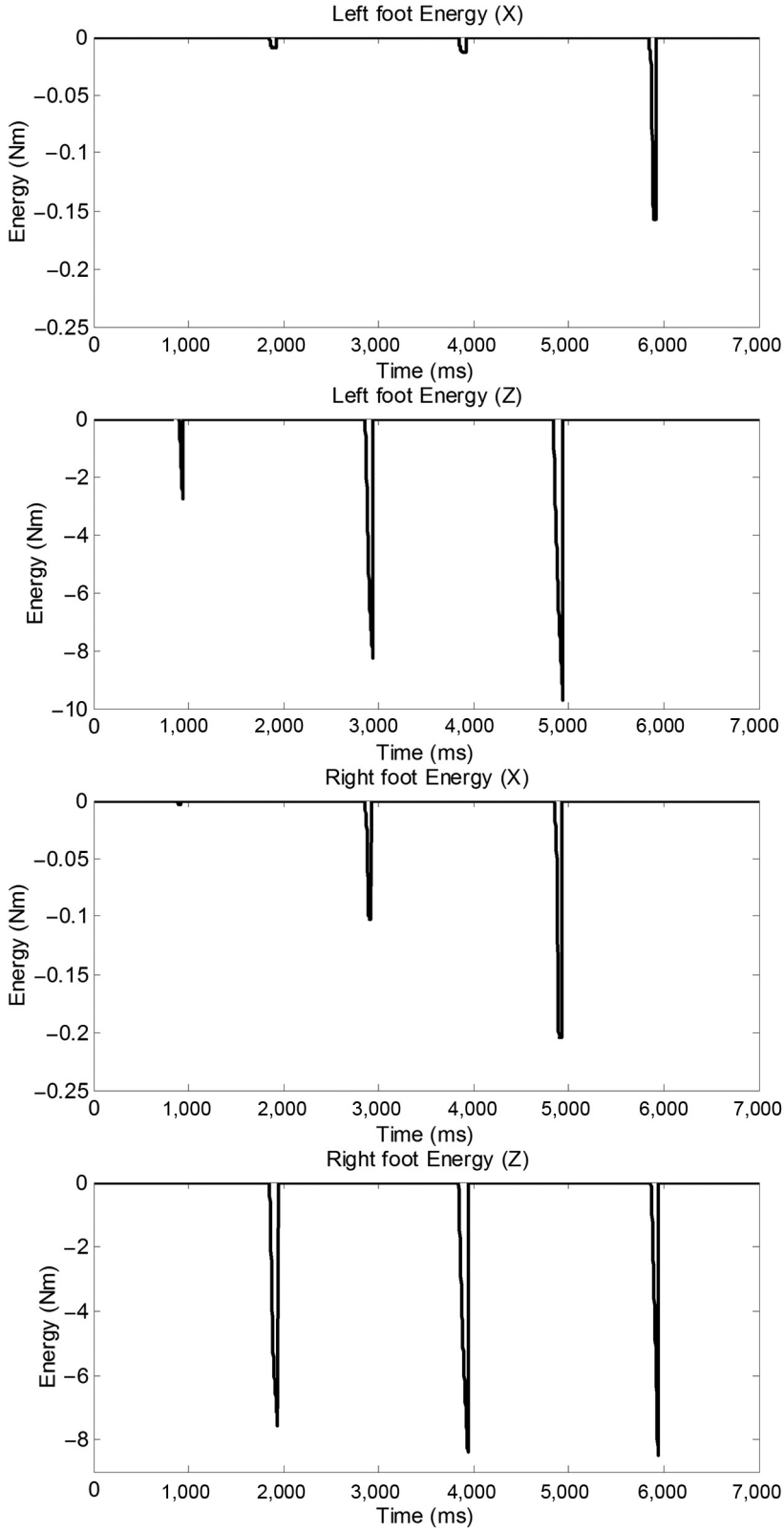

Figure 19 The reaction forces with on-line modification for the slope

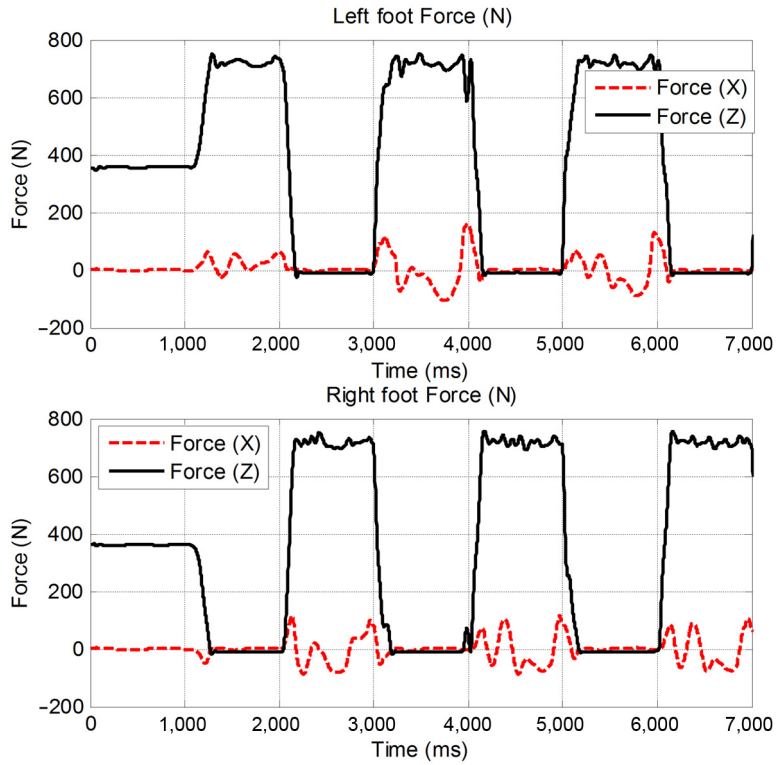

Figure 20 The energy with on-line modification for the uneven terrain

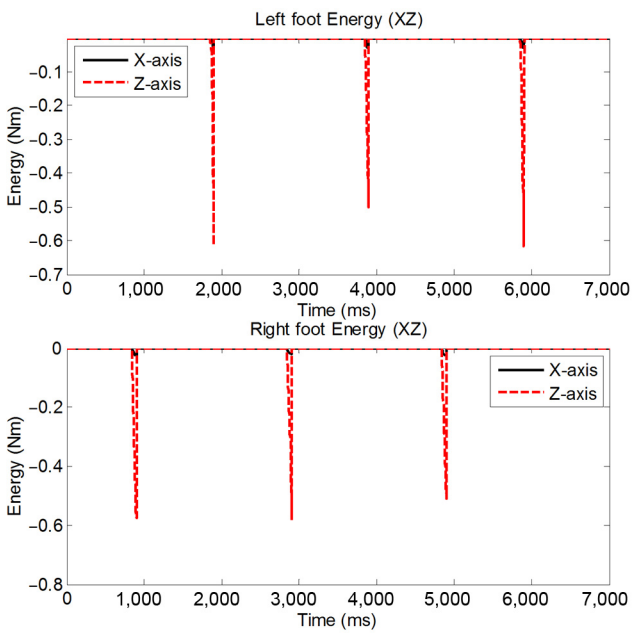

Figure 21 The output of PO/PCs ($\Delta \boldsymbol{p}_{pc}$) by the PO/PCs method for the uneven terrain

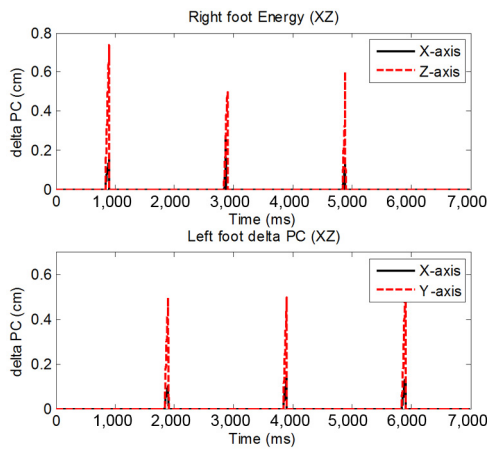

maximum value of the impulsive force was approximately −260 N. Along the z-axis, the maximum value of the impulsive force was approximately 1,100 N, and it was 1.46 times the biped robot's weight. Figure 18 shows the input energies from three-ports biped robot's foot without on-line modification for the uneven terrain. Along the x-axis, big negative energies only appeared when the swing foot landed on the badly rough terrain, which owes to the trajectories preplanning strategy.

Figures 19–22 show the results for the uneven terrain when on-line modification based on extended time-domain passivity control was used. Compared with the no on-line modification, the proposed control strategy has also improved the performance of bipedal walking on the uneven terrain. The biped robot's foot landed on the uneven terrain surface without impulsive forces, and the scale of negative energies was decreased by 10-20 times compared to the no on-line modification control. In

Figure 22 The decomposed position trajectories of the feet with on-line modification for the slope

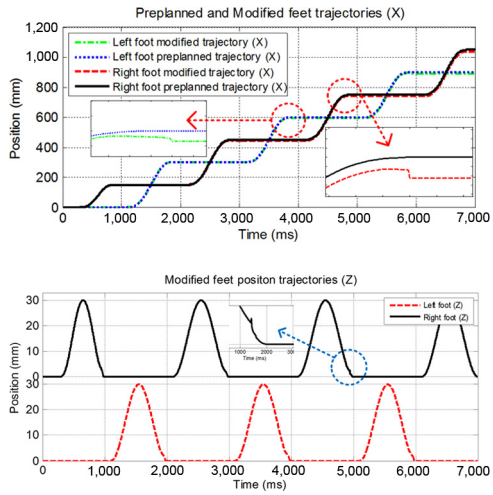

addition, the biped robot's foot was slightly moved upward along the z-axis and backward along the x-axis on each landing time according to the outputs $\Delta \boldsymbol{p}_{pc}$ of the PCs as shown in Figure 21, so the real walking distance slightly less than the preplanned walking distance, as shown in Figure 22.

The results of the overall experiments have demonstrated that the proposed soft landing control scheme suppresses the impulsive landing forces on the slope and the uneven terrain and makes stable foot landing possible. The dynamic equations of the biped robot and ground environment are not used anywhere in the proposed control strategy. Also note that the proposed strategy is not limited to the slope and uneven terrain; it can be used in all terrains.

5. Conclusion

This paper proposed a soft landing control strategy to avoid and absorb the impulsive ground reaction forces for enhancing the biped walking stability. The proposed strategy is composed of off-line preplanning and on-line modification of the trajectories of the swing foot. For off-line preplanning, the preplanning trajectories could avoid effectively the reaction force in the working direction or in the normal direction of the body plane. For on-line modification, the position trajectories of the swing foot were real-time modified slightly to suppress the impulsive landing forces using the extended time-domain passivity control approach. The effectiveness of the proposed soft landing control strategy was demonstrated by carrying dynamical bipedal walking experiment on the slope and the uneven terrain with the biped robot DRC-XT.

References

Choi, Y., Kim, D., Oh, Y. and You, B.J. (2007), "Posture/walking control for humanoid robot based on kinematic resolution of CoM Jacobian with embedded motion", *IEEE Transactions on Robotics*, Vol. 23 No. 6, pp. 1285-1293.

Hannaford, B. and Ryu, J.H. (2002), "Time-domain passivity control of haptic interfaces", *IEEE Transactions on Robotics and Automation*, Vol. 18 No. 1, pp. 1-10.

Huang, Q. and Nakamura, Y. (2005), "Sensory reflex control for humanoid walking", *IEEE Transactions on Robotics and Automation*, Vol. 21 No. 5, pp. 997-984.

Huang, Q., Yokoi, K., Kajita, S. and Kaneko, K. (2001), "Planning walking patterns for a biped robot", *IEEE Transactions on Robotics and Automation*, Vol. 17 No. 3, pp. 280-289.

Kajita, S., Kanehiro, F., Kaneko, K., Yokoi, K. and Hirukawa, H. (2001), "The 3D linear inverted pendulum mode: a simple modeling for a biped walking pattern generation", *Proceedings of IEEE International Conference on Intelligent Robots and Systems*, Vol. 1 No. 3, pp. 239-246.

Kim, Y.D., Lee, B.J., Ryu, J.H. and Kim, J.H. (2007), "Landing force control for humanoid robot by time-domain passivity approach", *IEEE Transactions on Robotics*, Vol. 23 No. 6, pp. 1294-1301.

Li, T.H.S., Su, Y.T., Lai, S.W. and Hu, J.J. (2011), "Walking motion generation, synthesis, and control for biped robot by using PGRL, LPI and fuzzy logic", *IEEE Transactions on Systems, Man, and Cybernetics, Part B (Cybernetics)*, Vol. 41 No. 3, pp. 736-748.

Li, T.H.S., Su, Y.T., Liu, S.H., Hu, J.J. and Chen, C.C. (2012), "Dynamic balance control for biped robot walking using sensor fusion, Kalman filter, and fuzzy logic", *IEEE Transactions on Industrial Electronics*, Vol. 59 No. 11, pp. 4394-4408.

Lim, H.O., Setiawan, S. and Takanishi, A. (2004), "Position-based impedance control of a biped humanoid robot", *Advanced Robotics*, Vol. 18 No. 4, pp. 415-435.

Motoi, N., Suzuki, T. and Ohnishi, K. (2009), "A bipedal locomotion planning based on virtual linear inverted pendulum mode", *IEEE Transactions on Industrial Electronics*, Vol. 56 No. 1, pp. 54-61.

Park, J.H. (2001), "Impedance control for biped robot locomotion", *IEEE Transactions on Robotics and Automation*, Vol. 17 No. 6, pp. 870-882.

Ryu, J.H., Kwon, D.S. and Hannaford, B. (2004), "Stability guaranteed control: time domain passivity approach", *IEEE Transactions on Control Systems Technology*, Vol. 12 No. 6, pp. 860-868.

Sato, T., Sakaino, S., Ohinishi, K. (2011), "Real-time walking trajectory generation method with three-mass models at constant body height for three-dimensional biped robots", *IEEE Transactions on Industrial Electronics*, Vol. 58 No. 2, pp. 376-383.

Shibata, M. and Natori, T. (2000), "Impact force reduction for biped robot based on decoupling COG control scheme", *Proceedings of IEEE International Workshop on Advanced Motion Control, Nagoya*, pp. 612-617.

Shimmyo, S., Sato, T. and Ohinishi, K. (2013), "Biped walking pattern generation by using preview control based on three-mass model", *IEEE Transactions on Industrial Electronic*, Vol. 61 No. 3, pp. 5137-5147.

Silva, F. and Machado, J. (2000), "Position/force control of biped walking robots", *Proceedings of IEEE International Conference on Systems, Man and Cybernetics, Nashville, TN*, Vol. 5, pp. 3288-3293.

Yamaguchi, J., Kinoshita, N., Takanishi, A. and Kato, I. (1996), "Development of a dynamic biped walking system for humanoid development of a biped walking robot adapting to the humans' living floor", *Proceedings of IEEE International Conference on Robotics and Automation, Minneapolis, MN*, Vol. 1, pp. 232-239.

Corresponding author

Hongbo Zhu can be contacted at: zhbkd@mail.ustc.edu.cn